doi:10.1093/brain/awu043 Brain 2014: 137; 1550–1561 | 1550

BRAIN
A JOURNAL OF NEUROLOGY

Association of brain amyloid-β with cerebral perfusion and structure in Alzheimer's disease and mild cognitive impairment

Niklas Mattsson,[1,2,3] Duygu Tosun,[1,3] Philip S. Insel,[1,3] Alix Simonson,[1,3] Clifford R Jack Jr,[4] Laurel A. Beckett,[5] Michael Donohue,[6] William Jagust,[7] Norbert Schuff[1,3] and Michael W. Weiner[1] on behalf of the Alzheimer's Disease Neuroimaging Initiative*

1 Department of Veterans Affairs Medical Centre, Centre for Imaging of Neurodegenerative Diseases, San Francisco, CA, USA
2 Clinical Neurochemistry Laboratory, Institute of Neuroscience and Physiology, the Sahlgrenska Academy at the University of Gothenburg, Mölndal, Sweden
3 Department of Radiology and Biomedical Imaging, University of California, San Francisco, CA, USA
4 Department of Radiology, Mayo Clinic, Rochester, MN, USA
5 Division of Biostatistics, Department of Public Health Sciences, School of Medicine, University of California, Davis, USA
6 Division of Biostatistics and Bioinformatics, Department of Family and Preventive Medicine, University of California, San Diego, La Jolla, CA, USA
7 Helen Wills Neuroscience Institute and School of Public Health, University of California, Berkeley, CA, USA

*For details see Appendix 1

Correspondence to: Niklas Mattsson, MD, PhD,
Department of Veterans Affairs Medical Centre,
Centre for Imaging of Neurodegenerative Diseases,
San Francisco, CA, USA
E-mail: niklas.mattsson@neuro.gu.se

Patients with Alzheimer's disease have reduced cerebral blood flow measured by arterial spin labelling magnetic resonance imaging, but it is unclear how this is related to amyloid-β pathology. Using 182 subjects from the Alzheimer's Disease Neuroimaging Initiative we tested associations of amyloid-β with regional cerebral blood flow in healthy controls ($n = 51$), early ($n = 66$) and late ($n = 41$) mild cognitive impairment, and Alzheimer's disease with dementia ($n = 24$). Based on the theory that Alzheimer's disease starts with amyloid-β accumulation and progresses with symptoms and secondary pathologies in different trajectories, we tested if cerebral blood flow differed between amyloid-β-negative controls and -positive subjects in different diagnostic groups, and if amyloid-β had different associations with cerebral blood flow and grey matter volume. Global amyloid-β load was measured by florbetapir positron emission tomography, and regional blood flow and volume were measured in eight *a priori* defined regions of interest. Cerebral blood flow was reduced in patients with dementia in most brain regions. Higher amyloid-β load was related to lower cerebral blood flow in several regions, independent of diagnostic group. When comparing amyloid-β-positive subjects with -negative controls, we found reductions of cerebral blood flow in several diagnostic groups, including in precuneus, entorhinal cortex and hippocampus (dementia), inferior parietal cortex (late mild cognitive impairment and dementia), and inferior temporal cortex (early and late mild cognitive impairment and dementia). The associations of amyloid-β with cerebral blood flow and volume differed across the disease spectrum, with high amyloid-β being associated with greater cerebral blood flow reduction in controls and greater volume reduction in late mild cognitive impairment and dementia. In addition to disease stage, amyloid-β pathology affects cerebral blood flow across the span from controls to dementia patients. Amyloid-β pathology has different associations with cerebral blood flow and volume, and may cause more loss of blood flow in early stages, whereas volume loss dominates in late disease stages.

Received October 7, 2013. Revised January 13, 2014. Accepted January 14, 2014. Advance Access publication March 12, 2014

Keywords: Alzheimer's disease; beta-amyloid; PET imaging; perfusion imaging; magnetic resonance imaging

Abbreviations: ADNI = Alzheimer's Disease Neuroimaging Initiative; ASL = arterial spin labelling; CBF = cerebral blood flow; MCI = mild cognitive impairment

Introduction

Alzheimer's disease is the most common cause of dementia, and is associated with accumulation of amyloid-β, tau, and progressive brain atrophy (Blennow *et al*., 2006). Early in the development of Alzheimer's disease, brain function in specific regions is reduced, as reflected by regionally reduced glucose metabolism (Friedland *et al*., 1983, 1989; Reiman *et al*., 1996; Silverman *et al*., 2001; Chételat *et al*., 2003; Mosconi *et al*., 2005, 2008) and cerebral blood flow (CBF) (Johnson *et al*., 1987; Ishii *et al*., 1997) measured by PET. Moreover, brain accumulation of amyloid-β is associated with both brain atrophy and CBF changes, as detected by ^{15}O-H_2O PET in cognitively healthy controls (Sojkova *et al*., 2008). However, several issues concerning the relationship between brain amyloid-β, brain atrophy and CBF remain elusive, especially the effects of amyloid-β on brain structure and perfusion at different levels of cognitive impairment. In this study, we aimed to determine the relationship between brain amyloid-β load, regional CBF reduction, and brain atrophy, across a wide spectrum of cognitive function.

CBF mapping can be accomplished using MRI-based arterial spin labelling (ASL), which uses magnetically labelled endogenous arterial blood water as a tracer for blood flow (Detre *et al*., 1992; Roberts *et al*., 1994). ASL-MRI is completely non-invasive and does not rely on ionizing radiation as does CBF mapping with approaches like ^{15}O-H_2O PET and Technetium-99m single photon emission computed tomography. Furthermore, ASL-MRI can be obtained in <10 min as part of a standard MRI protocol, and is easily co-registered to the structural MRI, facilitating analysis. Several studies have found that CBF measured by ASL is reduced in patients with Alzheimer's disease or mild cognitive impairment (MCI), especially in temporal-parietal and posterior cingulate cortices (Alsop *et al*., 2000, 2010; Schuff *et al*., 2009; Alexopoulos *et al*., 2012; Binnewijzend *et al*., 2013), and these changes often (Johnson *et al*., 2005), but not always (Wolk and Detre, 2012), co-localize with fluorodeoxyglucose PET patterns of hypometabolism. No previous study has examined ASL-CBF in relation to brain amyloid-β load, and no studies have compared the associations of amyloid-β load with brain perfusion and structure. Several structural MRI studies have found a strong association between brain atrophy and amyloid-β burden (Archer *et al*., 2006; Chételat *et al*., 2010). Therefore, another focus of this study was to relate the CBF alterations as detected with ASL to structural brain alterations in subjects with and without amyloid-β burden.

Specifically, we tested the following hypotheses: (i) brain amyloid-β (determined by florbetapir PET) is associated with CBF variations across the cognitive spectrum from healthy controls, to early MCI, late MCI and Alzheimer's disease with dementia; (ii) amyloid-β positive subjects across the cognitive spectrum groups show reduced CBF compared with amyloid-β negative controls, consistent with the theory that Alzheimer's disease starts with amyloid-β pathology in cognitively normal people, and progresses with development of other pathologies and clinical symptoms (Hardy and Selkoe, 2002; Jack *et al*., 2013); and (iii) brain amyloid-β has different associations with regional CBF and structure, consistent with the view that amyloid-β pathology leads to divergent functional and structural brain changes at different stages of Alzheimer's disease (Jack *et al*., 2013).

Materials and methods

Study design

Data used in the preparation of this article were obtained from the Alzheimer's Disease Neuroimaging Initiative (ADNI) database (adni.loni.usc.edu). The principal investigator of this initiative is Michael W. Weiner, MD, VA Medical Centre and University of California San Francisco. The ADNI is the result of efforts of many co-investigators from a broad range of academic institutions and private corporations, and subjects have been recruited from over 50 sites across the USA and Canada. The data used in this study were acquired in ADNI-2. Up-to-date information can be found at www.adni-info.org.

Participants

Our study population consisted of subjects from the ADNI-2 ASL substudy; the sample size and demographic characteristics of the subjects are listed in Table 1. Inclusion/exclusion criteria are described in detail at www.adni-info.org. Briefly, all subjects included in ADNI-2 were between the ages of 55 and 90 years, had completed at least 6 years of education, were fluent in Spanish or English, and were free of any significant neurological disease other than Alzheimer's disease. Control subjects had Mini-Mental State Examination score $\geqslant 24$, and Clinical Dementia Rating scale score 0. Subjects with early MCI had Mini-Mental State Examination score $\geqslant 24$, objective memory loss as shown on scores on delayed recall of the Wechsler Memory Scale Logical Memory II [0.5–1.5 standard deviations (SD) below the normal mean], Clinical Dementia Rating scale 0.5, preserved activities of daily living, and absence of dementia. Subjects with late MCI shared the early MCI criteria, but had greater objective memory loss measured by scores on delayed recall (>1.5 SD below the normal mean). Subjects with Alzheimer's disease dementia fulfilled the National Institute of Neurological and Communicative Disorders and Stroke and the Alzheimer's Disease and Related Disorders Association criteria for probable Alzheimer's disease, had Mini-Mental State Examination scores between 20–26 and a Clinical Dementia Rating scale of 0.5 or 1.0.

Arterial spin labelling magnetic resonance imaging acquisition

Details of ASL MRI data acquisition and processing are available online at www.loni.usc.edu. In short, ASL MRI was performed on 3.0 T

Table 1 Group demographics

Group	Control subjects	Early MCI	Late MCI	Alzheimer's disease	Total
n	51	66	41	24	182
Sex, M:F (% F)	21:30 (41%) *P* = 0.92	42:24 (64%) *P* = 0.30	17:24 (42%) *P* = 0.33	13:11 (54%) *P* = 0.03	90:92 (50%) *P* = 0.79
Age, years, mean, (SD)	72.2 (6.8) *P* = 0.044	70.1 (6.8) *P* = 0.0007	72.4 (8.2) *P* = 0.52	73.5 (5.6) *P* = 0.18	71.7 (7.1) *P* = 0.012
Education, years (mean, SD)	16.6 (2.4) *P* = 0.17	16.7 (2.7) *P* = 0.77	16.4 (2.7) *P* = 0.62	16.4 (2.2) *P* = 0.26	16.6 (2.5) *P* = 0.22
APOE ε4, + : − (% +)	14:35 (29%) *P* = 0.17	25:40 (39%) *P* = 0.0013	16:24 (39%) *P* = 0.0001	17:5 (77%) *P* = 0.46	72:103 (41%) *P* = 3e-9
MMSE, mean (SD)	29.0 (1.2) *P* = 0.053	28.8 (2.0) *P* = 0.016	27.7 (2.0) *P* = 0.001	23.5 (1.9) *P* = 0.83	28.0 (2.3) *P* = 2e-10

P-values are for associations with each variable and amyloid-β standardized uptake value ratio (continuous), tested by Spearman correlation [age, education, Mini-Mental State Examination (MMSE)] or Mann-Whitney U-test (sex, *APOE* genotype).

magnetic resonance machines from a single vendor (MAGNETOM Trio, Verio and Skyra, Siemens) using a pulsed ASL method (QUIPS II with thin-slice TI1 periodic saturation) with echo-planar imaging (Luh *et al*., 1999). Imaging parameters of the ASL scan were: field of view 256 mm, matrix 64 × 64, repetition time 3400 ms, echo time 12 ms, inversion time of arterial spins (TI1) 700 ms, total transit time of the spins (TI2) 1900 ms, tag thickness 100 mm, tag to proximal slice gap 25.4 mm, 24 axial slices, slice thickness 4 mm, time lag between slices 22.5 ms.

Arterial spin labelling magnetic resonance imaging preprocessing

All ASL images were preprocessed using a largely automated pipeline. Motion correction was done by alignment of each frame to the first in the sequence by rigid body transformation, using SPM8. Perfusion weighted images were computed by taking the difference between the mean-tagged and the mean-untagged ASL image. The first untagged ASL image (providing a fully relaxed MRI signal) was used as a reference image of the water density and used to calibrate the ASL signal for computing CBF and to estimate the transformation to co-register ASL MRI and structural MRI as explained later. The perfusion weighted images were intensity scaled to account for signal decay during acquisition and to provide intensities in physical units of CBF. The reference image was intensity scaled to provide a proxy for blood water magnetization.

Geometric distortion correction and structural to arterial spin labelling magnetic resonance imaging co-registration

Echo-planar imaging-based ASL images are more susceptible than structural images to non-linear geometric distortions. To accomplish registrations between CBF and structural MRI maps, linear transformations with nine degrees of freedom based on normalized mutual information were augmented by a non-linear registration approach based on total variance as described in detail in Tao *et al*. (2009). Furthermore, simulated T_2-weighted images derived from the corresponding T_1 image were used as intermediate maps in the co-registration step to reduce differences in contrast between ASL and structural MRI (details available online at www.loni.usc.edu). After correction for geometric distortions, the ASL images were aligned to structural T_1 images.

Arterial spin labelling magnetic resonance imaging partial volume correction

The analysis aimed to measure blood flow in primarily grey matter tissue. To correct for partial grey/white matter volume effects, the scaled perfusion weighted image intensities were adjusted according to a linear model of grey and white matter contributions to the ASL signal and based on probabilistic segmentation of grey and white matter densities in each MRI voxel. Adjustments were made assuming a constant ratio between grey matter and white matter perfusion (2.5 times greater in grey matter) and the scaled reference image was adjusted assuming constant ratios between grey matter and water (0.78), white matter and water (0.65), and CSF and water (0.97).

Computation of cerebral blood flow

The scaled, distortion corrected, co-registered and partial volume corrected perfusion weighted images were normalized to the reference image (i.e. an estimate of blood water magnetization) to express the ASL signal in physical units of arterial water density as CBF (ml/100 g × 60 s). This normalization also eliminates spatial B1-inhomogenity, as both maps are subject to the same B1-inhomogenity distribution.

Structural magnetic resonance imaging acquisition

Structural MRI was obtained using the same magnetic resonance machines as ASL with the standardized ADNI-2 protocol, available online (www.loni.usc.edu). In short, a T_1-weighted 3D MPRAGE sequence was used (repetition time 2300 ms, echo time 2.98 ms, flip angle 9°, field of view 256 mm, resolution 1.1 × 1.1 × 1.2 mm^3).

Regions of interest

FreeSurfer (surfer.nmr.mgh.harvard.edu) was used to generate anatomical region of interest statistics for CBF and volume. All images underwent manual quality control checks by trained staff for image quality and successful co-registration. In this study we tested eight *a priori* designated regions of interest, where seven are suspected to be vulnerable to Alzheimer's disease (entorhinal, inferior temporal, hippocampal, inferior parietal, posterior cingulate, precuneus, and medial-orbitofrontal cortices) and one was used as a control region (pericalcarine), where we expected no changes in Alzheimer's disease. Data of the right and left hemispheres were averaged. To reduce contributions from noisy ASL signals in regions of major tissue loss, we used a threshold of $>70\%$ structural voxel count for the inclusion of ASL regions. In the regression models for estimations of CBF and volume data, the precentral cortex and the total intracranial volume, respectively, were used as reference regions.

Florbetapir positron emission tomography

PET image data were acquired and processed as described previously (Landau *et al*., 2012). Full protocols are online (adni.loni.usc.edu). In sum, florbetapir image data were acquired 50 to 70 min post-injection. Images were reconstructed immediately following the scan, and repeat scans were acquired if motion artefact was detected. For quantification of florbetapir, 3 T 3D MPRAGE MRI scans were used. MRI images were segmented and parcellated into individual cortical regions with FreeSurfer, and used to extract mean florbetapir uptake (standardized uptake value ratio) from grey matter within lateral and medial frontal anterior, posterior cingulate, lateral parietal, and lateral temporal regions relative to uptake in the whole cerebellum (white and grey matter). The overall cortical mean standardized uptake value ratio from these regions combined was used for each subject in all amyloid-β analyses in this study. We did not use data on regional amyloid-β load for the statistical analyses in this study.

Statistical analyses

We evaluated associations between demographic factors, amyloid-β load and CBF by non-parametric tests (Spearman's correlation and Mann-Whitney U test, as appropriate). To validate the present data set and confirm previous findings of Alzheimer's disease-dependent CBF-reductions, we tested for overall differences in CBF between diagnostic groups by linear regression models with regional CBF as the dependent variable and group as the independent variable, accounting for age, sex and reference CBF (precentral cortex CBF). After this, we conducted three different statistical analyses, according to the three hypotheses:

(i) We tested for overall statistical effects of amyloid-β on CBF by linear regression models with regional CBF as the dependent variable and amyloid-β standardized uptake value ratio as the independent (continuous) variable, across all study subjects simultaneously. Likelihood ratio tests were used to identify diagnosis-dependent differences in the relationship between CBF and amyloid-β in each region by contrasting two models, one with an amyloid-β by diagnosis interaction term and the other without this interaction term, while the other factors in the models were kept the same.

(ii) Based on the amyloid cascade hypothesis and the dynamic biomarker model, we assumed that amyloid-β negative controls represented the best reference group to identify statistical effects associated with development of Alzheimer's disease. We therefore dichotomized each diagnostic group by amyloid-β (using a previously established amyloid-β standardized uptake value ratio cut-off for amyloid-β load, $\geqslant 1.11$), and tested for differences between amyloid-β negative controls and amyloid-β positive subjects (grouped by controls, early MCI, late MCI and Alzheimer's disease) or other amyloid-β negative subjects [grouped by early MCI and late MCI, the few amyloid-β negative Alzheimer's disease cases ($n = 4$) were excluded from this analysis]. For this we used linear regression models with 'Group' as the independent variable (amyloid-β negative controls was the reference group).

(iii) Finally, we performed similar tests for structural volume and compared statistical effects of amyloid-β and diagnosis on CBF and volume. To test if amyloid-β had different associations with CBF and volume within diagnostic groups, we used linear mixed effects models after concatenating the two response vectors and including an interaction between a factor for imaging modality (CBF versus volume) and amyloid-β, as a predictor. Before concatenation, CBF was adjusted for the effect of the reference CBF region by way of residualization from linear regression. Similarly, volumes were adjusted for intracranial volume. CBF and volume data were then centred and scaled by the estimated error from the regressions in the residualization step. The final models included interactions between imaging modality and amyloid-β, age, and sex as predictors, plus both main effects. All models included a random intercept and a random term for imaging modality. We extracted the statistical effects of amyloid-β on CBF and volume, and the effect of the interaction between amyloid-β and imaging modality. Finally, we performed similar tests using the combined diagnostic group and amyloid-β status as predictor instead of continuous amyloid-β (amyloid-β negative controls versus each of amyloid-β positive controls, early MCI, late MCI and Alzheimer's disease).

The statistical tests are summarized in Supplementary Table 1. All linear regression models were co-varied for age, sex and reference CBF or intracranial volume (for structural data). Because *APOE* ε4 allele status and amyloid-β load are so highly correlated, models were not adjusted for *APOE* genotype, although it is possible that *APOE* genotype and amyloid-β pathology may have independent statistical effects on CBF, which could warrant further studies. Significance was determined at $P < 0.05$. Corrections for multiple comparisons were done using false discovery rate correction. All statistics were done using R (v. 2.15.2, The R Foundation for Statistical Computing).

Results

The study included 51 control subjects, 66 patients with early MCI, 41 patients with late MCI and 24 patients with Alzheimer's disease (see Table 1 for demographic data). Differences in age and education between groups were not significant, but there was a strong trend of fewer males present in the early MCI group compared with other groups ($P = 0.051$, $\chi^2 = 7.78$, Pearson's chi-square test for sex in all groups). As expected, *APOE* ε4 prevalence was highest in patients with Alzheimer's disease, and intermediate in early and late MCI, whereas Mini-Mental State Examination score was lowest in patients with Alzheimer's disease.

Associations between demographic factors, amyloid-β and cerebral blood flow

Higher amyloid-β levels were associated with females (in Alzheimer's disease), higher age (in controls, early MCI and the whole cohort), *APOE* ε4 (in early MCI, late MCI and the whole cohort), and lower Mini-Mental State Examination score (in controls, early MCI, late MCI and the whole cohort) but not with education (Table 1). We tested associations between regional CBF and demographic factors in the whole study population. Age was positively correlated to higher CBF in inferior parietal ($P = 0.003$), posterior cingulate ($P = 0.003$), and medial-orbito frontal cortices ($P = 0.018$). Compared with males, females had higher CBF in inferior parietal ($P = 0.006$), precuneus ($P = 0.009$), and pericalcarine cortices ($P = 0.014$). *APOE* ε4 carriers had lower CBF in entorhinal ($P = 0.017$), inferior temporal ($P = 0.017$), and pericalcarine cortices ($P = 0.045$). Mini-Mental State Examination score was positively correlated to higher CBF in entorhinal ($P = 0.034$), hippocampus ($P = 0.028$), and inferior temporal ($P = 0.0072$) cortices. There were no significant associations between regional CBF and education.

Overall differences in cerebral blood flow between diagnostic groups

CBF was reduced in Alzheimer's disease compared with control subjects in most regions where we expected to see effects (entorhinal, $P < 0.01$; hippocampus, $P = 0.01$; inferior temporal, $P < 0.01$; inferior parietal, $P < 0.01$; posterior cingulate, $P = 0.07$; precuneus, $P < 0.01$; medial-orbito frontal, $P = 0.03$). In contrast, CBF differences were not significant in the control region (pericalcarine, $P = 0.27$). The effects were significant after correction for multiple comparisons in entorhinal ($P = 0.05$), inferior temporal ($P = 0.01$), inferior parietal ($P = 0.01$) and precuneus ($P = 0.01$) (corrected for eight tests). We found no significant differences in CBF between controls and early or late MCI. These data are presented in Supplementary Fig. 1 and Supplementary Table 2.

Overall associations of brain amyloid-β with cerebral blood flow

Increased whole brain amyloid-β load had associations with reduced CBF in the entorhinal ($P < 0.001$), inferior temporal ($P < 0.001$), inferior parietal ($P < 0.001$) and precuneus cortices ($P = 0.010$) (Fig. 1). In contrast, in posterior cingulate, there was a trend towards a positive correlation, meaning CBF increase with higher amyloid-β load ($P = 0.061$). There were no associations between CBF and amyloid-β load in the medial-orbitofrontal or pericalcarine cortices. All significant effects remained significant after correcting for multiple comparisons using false discovery rate correction (corrected for eight tests).

Diagnosis dependent associations of brain amyloid-β with cerebral blood flow

Likelihood ratio tests of differences in the relationship between CBF and amyloid-β load across diagnostic groups were non-significant in entorhinal, hippocampal, inferior temporal, inferior parietal, posterior cingulate and precuneus cortices ($P = 0.29$ to $P = 0.85$) (Fig. 1). However, in several regions, patients with Alzheimer's disease showed an opposite pattern compared with the other groups, with CBF increasing with high amyloid-β load. This was most evident in the inferior parietal cortex, where the likelihood ratio test indicated a difference between the diagnostic groups ($P = 0.05$). There were no significant differences between groups when correcting for multiple comparisons using false discovery rate correction (corrected for eight tests).

Differences in cerebral blood flow compared with amyloid-β-negative control subjects

As it is possible that Alzheimer's disease starts in amyloid-β-negative cognitively normal subjects, and then develops into amyloid-β-positive preclinical disease and finally into amyloid-β-positive symptomatic disease, we compared CBF in amyloid-β-negative control subjects with amyloid-β-positive controls, early MCI, late MCI and Alzheimer's disease. According to the amyloid cascade hypothesis and the dynamic biomarker model, amyloid-β-negative early and late MCI are likely to constitute non-Alzheimer's disease, and these groups were also compared with amyloid-β-negative controls. For this analysis we dichotomized the groups by brain amyloid-β standardized uptake value ratio (cut-off $\geqslant 1.11$). We excluded the few subjects with Alzheimer's disease ($n = 4$) who were amyloid-β-negative by this definition. We used linear regression with group (diagnosis combined with amyloid-β-category) as the independent variable (Fig. 2). Compared with amyloid-β-negative controls, we found nominally significantly reduced CBF in amyloid-β-positive Alzheimer's disease (in entorhinal, hippocampal, inferior temporal, inferior parietal, and precuneus cortices), amyloid-β-positive late MCI (in inferior parietal and inferior temporal cortices), amyloid-β-positive early MCI (inferior temporal cortex), and amyloid-β-negative early MCI (posterior cingulate). When correcting for multiple comparisons using false discovery rate correction (corrected for 48 tests), effects were significant in inferior temporal (Alzheimer's disease), inferior parietal (late MCI and Alzheimer's disease) and precuneus (Alzheimer's disease) cortices.

Associations of amyloid-β with volume and cerebral blood flow

As expected, there were significantly smaller regional grey matter volumes in late MCI and Alzheimer's disease compared with control subjects in entorhinal ($P < 0.01$), inferior temporal (late MCI, $P = 0.02$, Alzheimer's disease, $P < 0.01$), inferior parietal (late MCI, $P = 0.02$, Alzheimer's disease, $P < 0.01$), and hippocampal

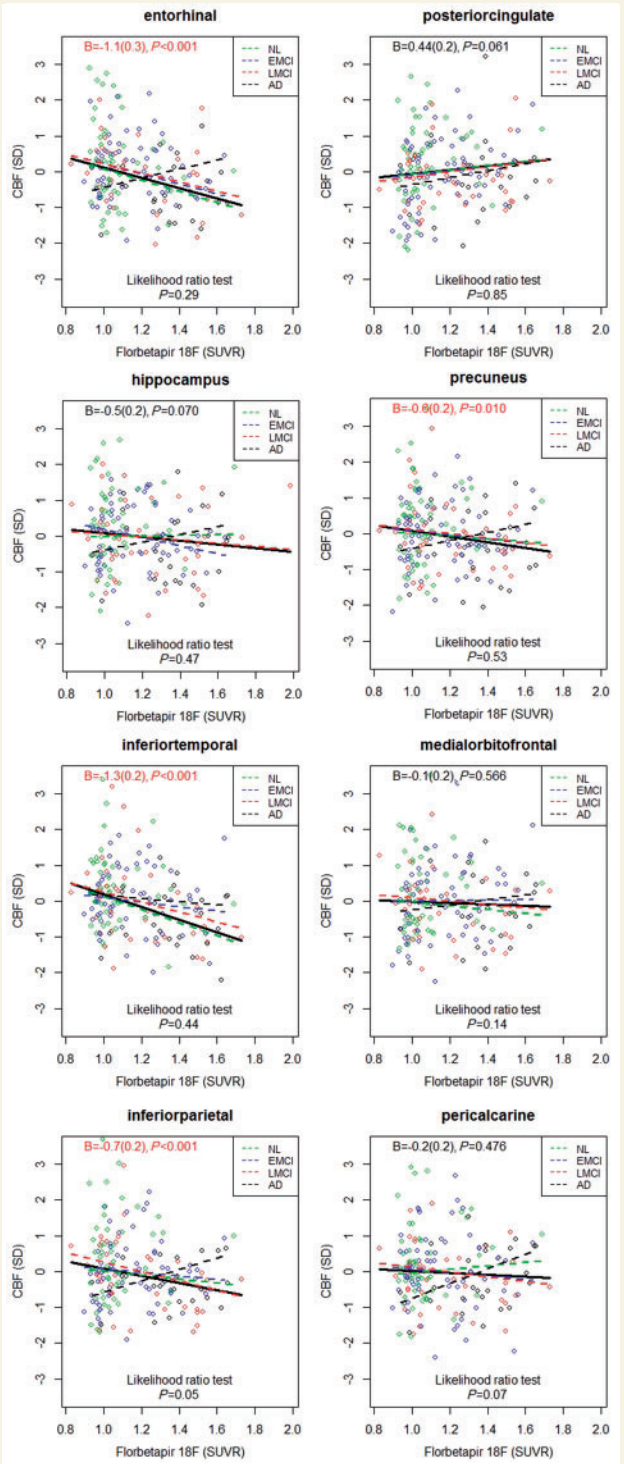

Figure 1 Associations between cerebral blood flow and amyloid-β load. CBF values were centred and standardized. Associations were tested simultaneously in healthy controls (NL, green), early and late MCI (EMCI, blue, and LMCI, red, respectively), and Alzheimer's disease dementia (AD, black). The fitted lines are from linear regression models, co-varied for age, sex and CBF in a reference region (precentral cortex). The data in the top of each panel are the regression coefficients B (standard error) and *P*-values for amyloid-β standardized uptake value ratio (SUVR) in the linear regression models fitted for all subjects simultaneously (thick solid line). The dashed lines represent models fitted within diagnostic groups. Data in the bottom of each panel are for likelihood ratio tests, comparing linear regression models with and without the interaction between diagnostic groups and amyloid-β standardized uptake value ratio, to assess differences between diagnostic groups (a significant *P*-value suggests that the relationship between regional CBF and amyloid-β standardized uptake value ratio differs by diagnosis).

regions ($P < 0.01$), but not in posterior cingulate, precuneus, medial orbito-frontal and pericalcarine regions (Supplementary Fig. 2). There were no volume reductions in early MCI compared with controls [but subjects with early MCI had larger volumes in precuneus ($P = 0.01$) and pericalcarine ($P = 0.02$)]. High amyloid-β load was significantly associated with smaller volumes in entorhinal ($P < 0.001$), hippocampal ($P < 0.001$), inferior temporal ($P = 0.042$), inferior parietal ($P < 0.001$), and precuneus cortices ($P = 0.039$) across all diagnostic groups (indicated by the non-significant likelihood ratio tests for models with the interaction term amyloid-β by diagnosis compared to models without the interaction term, Supplementary Fig. 3). The only exception was in the hippocampus, where patients with Alzheimer's disease had a positive association between large volumes and high amyloid-β load (likelihood ratio test, $P = 0.02$).

In the last part of this study, we compared statistical effects of amyloid-β on CBF versus effects on brain structure. We first compared associations within the diagnostic groups of controls, early MCI and late MCI (Table 2), but not within Alzheimer's disease because of the small dynamic range of amyloid-β in subjects with Alzheimer's disease. In controls, the associations of amyloid-β with CBF and volume were different in entorhinal cortex ($P = 0.038$), where amyloid-β had a negative effect on CBF, but a positive effect on volume. Within early MCI and late MCI, we found no significant differences in associations of amyloid-β with CBF and volume. Finally, we compared the statistical effects of amyloid-β positivity and diagnosis on CBF and volume (comparing amyloid-β negative controls with amyloid-β positive controls, early MCI, late MCI, and Alzheimer's disease, Table 3). In mild disease stages, we found only minor differences between associations with CBF and volume, with a difference in amyloid-β positive controls in entorhinal cortex ($P = 0.021$), confirming the test with continuous amyloid-β described in the previous paragraph. In advanced disease stages, associations with volume dominated. Amyloid-β-positive patients with late MCI and Alzheimer's disease had larger reductions of volume than CBF in hippocampus (late MCI: $P = 0.053$, Alzheimer's disease: $P = 0.012$) and entorhinal cortex (late MCI: $P = 0.10$, Alzheimer's disease: $P = 0.017$). However, the different associations with CBF and volume were mild, and did not remain after correction for multiple comparisons.

Discussion

This study is the first to report statistical effects of brain amyloid-β accumulation on CBF measured by ASL MRI and to compare the

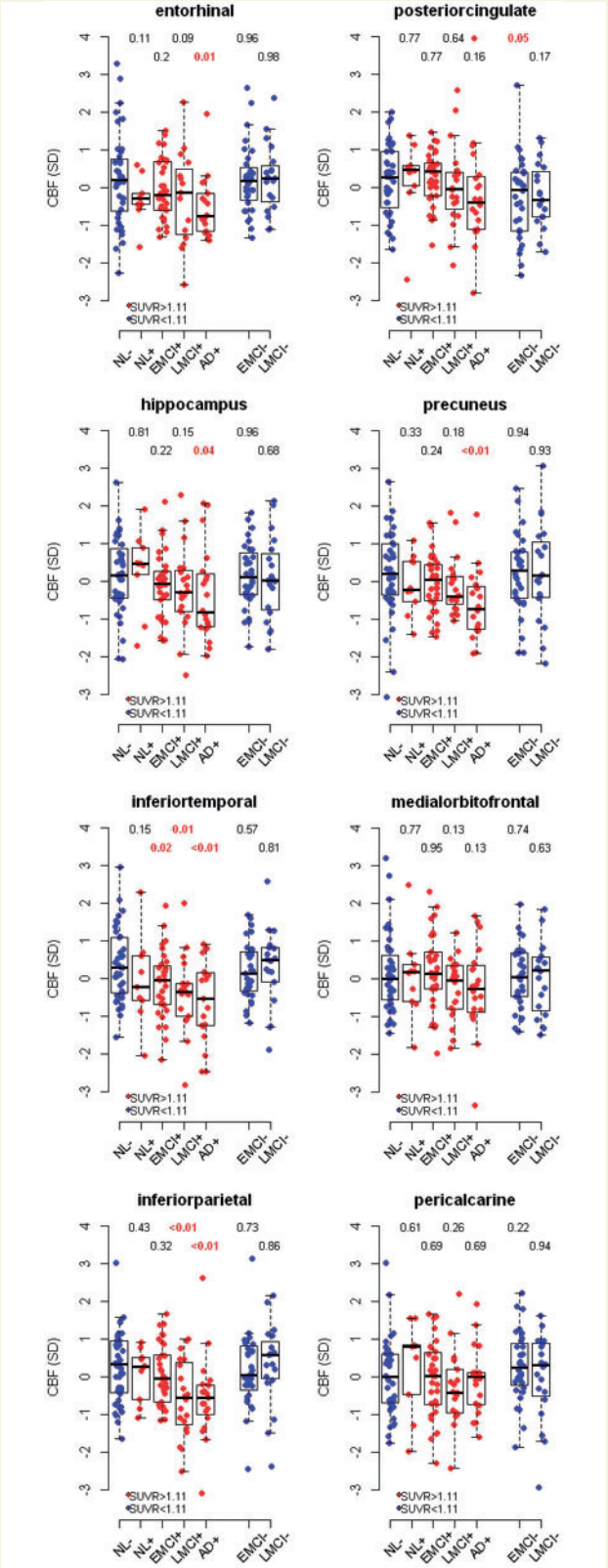

Figure 2 Effects of amyloid-β standardized uptake value ratio (SUVR) and diagnostic group on CBF. CBF values were adjusted for age, sex, and CBF in a reference region (precentral cortex), centered and standardized. Amyloid-β-negative healthy controls (NL) (dichotomized by amyloid-β standardized uptake value ratio $\geqslant$1.11) were compared with amyloid-β-positive controls, early and late MCI (EMCI and LMCI), and Alzheimer's disease dementia (AD), and with amyloid-β-negative early MCI and late MCI. Values above each column are *P*-values from linear regression models, for the combination of amyloid-β and diagnosis as predictor of CBF, co-varied for age, sex and reference CBF (precentral cortex). Shown *P*-values are not corrected for multiple comparisons.

effects on CBF with effects on brain structure. We found that (i) brain amyloid-β load was associated with reduced CBF in temporo-parietal regions across all subjects; (ii) amyloid-β positive subjects had reduced CBF in several regions compared with amyloid-β negative controls; and (iii) effects of brain amyloid-β load differed between CBF and volume, supporting the view that amyloid-β has stronger associations with brain function than with structure in mild disease stages, but larger associations with structure in advanced disease stages. We also replicated previous findings that CBF was significantly lower in temporo-parietal and frontal regions in patients with Alzheimer's disease than in control subjects (Alsop *et al.*, 2010). When not taking amyloid-β into account, we found no significant overall CBF reductions in early or late MCI when compared with control subjects, indicating that the CBF measurements were not sensitive enough to distinguish between these heterogeneous groups. This is in contrast to some other ASL studies (Johnson *et al.*, 2005; Xu *et al.*, 2007; Chao *et al.*, 2009; Dai *et al.*, 2009), and may be because of the heterogeneous nature of early and late MCI, where only a fraction of the subjects have amyloid-β pathology. In sum, our findings were consistent with our hypotheses, and support the use of ASL to characterize the relationship between amyloid-β pathology and CBF, especially in early stages of Alzheimer's disease, when brain function is probably more vulnerable to amyloid-β than is brain structure.

The first major finding of this study is that brain amyloid-β load was associated with reduced CBF in several Alzheimer's disease-related brain regions regardless of cognitive status, even when correcting for multiple comparisons. This is a novel finding, but it is in agreement with many previous reports of reduced perfusion in Alzheimer's disease or mild cognitive impairment, as measured by PET/single photon emission computed tomography (Johnson *et al.*, 1987; Ishii *et al.*, 1997; Dougall *et al.*, 2004; Matsuda, 2007; Alsop *et al.*, 2010) or ASL (Alsop *et al.*, 2000, 2010; Johnson *et al.*, 2005; Dai *et al.*, 2009; Binnewijzend *et al.*, 2013). No previous study has tested effects of amyloid-β on ASL CBF in mild cognitive impairment or healthy controls, but CBF has been shown to differ between amnestic versus dysexecutive mild cognitive impairment (Chao *et al.*, 2009), between progressive versus stable mild cognitive impairment (Chao *et al.*, 2010), and between *APOE* ε4-positive and -negative MCI (Kim *et al.*, 2013), which are results that may all have been influenced by amyloid-β pathology. The finding that amyloid-β load is associated with reduced CBF across the different diagnostic groups is in agreement with the concept that amyloid-β-positive subjects have Alzheimer's disease pathology, and that the controls, early

Table 2 Effects of brain amyloid-β on cerebral blood flow and volume within diagnostic groups

		Volume		CBF		Difference	
Groups	**Region**	**β**	***P***	**β**	***P***	**β**	***P***
Controls ($n = 51$)	**Entorhinal**	0.478	0.636	−1.867	0.067	**2.345**	**0.038**
	Hippocampus	−0.4	0.675	0.102	0.922	−0.502	0.661
	Inferior temporal	0.06	0.952	**−2.288**	**0.028**	2.349	0.102
	Inferior parietal	1.455	0.121	−1.186	0.218	2.64	0.054
	Posterior cingulate	0.216	0.815	1.15	0.258	−0.934	0.543
	Precuneus	−0.365	0.668	−0.635	0.525	0.27	0.848
	Medial orbito-frontal	0.723	0.483	−0.771	0.455	1.494	0.299
	Pericalcarine	0.998	0.329	0.661	0.519	0.337	0.808
Early MCI ($n = 66$)	Entorhinal	−0.634	0.408	**−1.537**	**0.043**	0.903	0.35
	Hippocampus	**−1.52**	**0.024**	−1.417	0.063	−0.103	0.922
	Inferior temporal	−0.018	0.98	−0.727	0.342	0.71	0.449
	Inferior parietal	−0.879	0.225	−0.8	0.291	−0.079	0.944
	Posterior cingulate	0.421	0.567	0.885	0.209	−0.464	0.639
	Precuneus	−0.602	0.422	−0.832	0.273	0.23	0.81
	Medial orbito-frontal	0.493	0.517	0.141	0.844	0.353	0.745
	Pericalcarine	0.241	0.749	−0.561	0.432	0.802	0.465
Late MCI ($n = 41$)	Entorhinal	**−1.757**	**0.012**	−1.276	0.083	−0.481	0.589
	Hippocampus	**−1.837**	**0.007**	−0.511	0.484	−1.326	0.171
	Inferior temporal	−0.988	0.193	**−1.787**	**0.014**	0.798	0.371
	Inferior parietal	**−2.207**	**0.001**	**−1.735**	**0.012**	−0.472	0.566
	Posterior cingulate	−0.861	0.244	0.871	0.234	−1.732	0.078
	Precuneus	−1.355	0.052	−0.825	0.257	−0.531	0.490
	Medial orbito-frontal	0.134	0.854	−0.604	0.407	0.738	0.464
	Pericalcarine	−0.83	0.279	−0.709	0.357	−0.12	0.902

Effects from linear mixed models, with CBF and volume as dependent variables (stacked), and brain amyloid-β standardized uptake value ratio as independent variable (continuous), co-varied for age and sex, in controls and early and late mild cognitive impairment (early MCI and late MCI). CBF and volume were residualized by reference CBF (precentral cortex) or intracranial volume, respectively. Differences in effects were compared by the interaction between amyloid-β and imaging modality. Tests significant at $P < 0.05$ are printed in bold. The effects were mild and generally not significant after correction for multiple comparisons using false discovery rate correction (corrected for 32 tests for volume and 32 for CBF; the only effect that remained significant was for amyloid-β on volume in inferior parietal cortex in late MCI, $P = 0.024$). No differences between effects on volume and CBF were significant when correcting for multiple comparisons (corrected for 32 tests).

MCI and late MCI groups are heterogeneous, containing varying extents of Alzheimer's disease pathology.

We found a tendency to a positive correlation between higher amyloid-β load and increased CBF in the posterior cingulate across all participants, and in several regions there were positive correlations between amyloid-β load and CBF in patients with Alzheimer's disease, although this was not seen in the other diagnostic groups. A few previous reports have found increased CBF in hippocampus or the medial temporal lobe in healthy elderly at familial and genetic risk for Alzheimer's disease (Fleisher *et al*., 2009; Bangen *et al*., 2012), and fluorodeoxyglucose PET hypermetabolism in relation to amyloid-β load in mild cognitive impairment (Cohen *et al*., 2009) and healthy controls (Ossenkoppele *et al*., 2013; Oh *et al*., 2014). Some, but not all, previous ASL studies have also found increased perfusion in Alzheimer's disease (or MCI or healthy controls at risk for Alzheimer's disease) in some regions, including insular cortex, temporal cortex, anterior cingulate, or subcortical structures such as hippocampus, amygdala and basal ganglia (Alsop *et al*., 2008; Dai *et al*., 2009; Fleisher *et al*., 2009; Alexopoulos *et al*., 2012). It should be noted that CBF is often but not always (Fink *et al*., 1996) coupled to the metabolic activity in the brain measured by fluorodeoxyglucose PET, and some studies have also found positive associations between fluorodeoxyglucose PET and brain amyloid-β load. These increases in perfusion and metabolism may either reflect mechanisms compensating for amyloid-β neurotoxicity, or suggest that amyloid-β accumulation itself is driven by increased neural activity (Cohen *et al*., 2009; Jagust and Mormino, 2011; Ossenkoppele *et al*., 2013). However, the fact that amyloid-β load was associated with CBF reductions in regions other than posterior cingulate gyrus may argue against amyloid-β accumulation resulting from increased neural activity.

The second major finding of this study is that when dichotomizing subjects by amyloid-β load and comparing amyloid-β-positive subjects within each diagnostic group with amyloid-β-negative controls, amyloid-β-positive subjects with early MCI, late MCI and Alzheimer's disease had reduced CBF in several regions. Although some of these associations were weak and did not remain after correcting for multiple comparisons, these results are in line with the theory that Alzheimer's disease starts with amyloid-β pathology in cognitively normal people, and progresses with neurodegeneration, reduced brain activity and clinical symptoms (Hardy and Selkoe, 2002; Jack *et al*., 2013). No previous study has compared ASL CBF between amyloid-β-positive subjects at different stages of cognitive impairment with amyloid-β-negative control subjects, but our results are consistent with findings using other biomarker modalities and study designs (Jack *et al*., 2011; Bateman *et al*., 2012). These findings add to

Table 3 Effects of amyloid-β positivity and diagnostic group on cerebral blood flow and volume

Groups	Region	Volume		CBF		Difference	
		β	*P*	β	*P*	β	*P*
Amyloid-β-negative control subjects (*n* = 41) versus amyloid-β-positive control subjects (*n* = 10)	**Entorhinal**	0.467	0.234	−0.552	0.171	**1.019**	**0.021**
	Hippocampus	−0.176	0.630	0.031	0.937	−0.207	0.637
	Inferior temporal	−0.181	0.661	−0.753	0.083	0.573	0.339
	Inferior parietal	0.309	0.395	−0.351	0.342	0.660	0.213
	Posterior cingulate	0.009	0.980	0.208	0.595	−0.200	0.735
	Precuneus	−0.104	0.750	−0.363	0.341	0.259	0.631
	Medial orbito-frontal	0.149	0.706	0.070	0.859	0.079	0.887
	Pericalcarine	0.554	0.180	0.139	0.739	0.415	0.46
Amyloid-β-negative control subjects (n = 41) versus amyloid-β-positive patients with early MCI (*n* = 33)	Entorhinal	−0.298	0.234	−0.254	0.314	−0.044	0.88
	Hippocampus	−0.184	0.424	−0.340	0.170	0.156	0.602
	Inferior temporal	−0.152	0.552	**−0.600**	**0.020**	0.448	0.177
	Inferior parietal	−0.294	0.199	−0.239	0.327	−0.055	0.868
	Posterior cingulate	0.065	0.781	0.111	0.656	−0.046	0.898
	Precuneus	0.163	0.502	−0.253	0.297	0.417	0.229
	Medial orbito-frontal	0.353	0.151	−0.003	0.991	0.356	0.286
	Pericalcarine	**0.515**	**0.035**	−0.076	0.757	0.591	0.096
Amyloid-β-negative control subjects (*n* = 41) versus amyloid-β-positive patients with late MCI (*n* = 21)	Entorhinal	**−0.904**	**0.002**	−0.37	0.234	−0.535	0.100
	Hippocampus	**−0.948**	**<0.001**	−0.275	0.330	−0.672	0.053
	Inferior temporal	**−0.655**	**0.021**	**−0.795**	**0.007**	0.139	0.688
	Inferior parietal	**−0.623**	**0.021**	**−0.789**	**0.004**	0.167	0.648
	Posterior cingulate	−0.104	0.714	−0.096	0.738	−0.008	0.985
	Precuneus	−0.149	0.569	−0.347	0.213	0.198	0.614
	Medial orbito-frontal	−0.096	0.739	−0.352	0.194	0.256	0.462
	Pericalcarine	0.512	0.079	−0.378	0.198	0.890	**0.031**
Amyloid-β-negative control subjects (*n* = 41) versus amyloid-β-positive patients with Alzheimer's disease (*n* = 20)	Entorhinal	**−1.319**	**<0.001**	**−0.594**	**0.036**	**−0.725**	**0.017**
	Hippocampus	**−1.209**	**<0.001**	−0.493	0.075	**−0.716**	**0.012**
	Inferior temporal	**−0.989**	**<0.001**	**−0.917**	**0.001**	−0.072	0.827
	Inferior parietal	**−0.857**	**0.001**	**−0.759**	**0.006**	−0.098	0.776
	Posterior cingulate	−0.437	0.102	−0.294	0.286	−0.143	0.714
	Precuneus	−0.430	0.100	**−0.731**	**0.006**	0.301	0.432
	Medial orbito-frontal	−0.437	0.115	−0.341	0.213	−0.096	0.792
	Pericalcarine	0.489	0.079	−0.161	0.568	0.651	0.104

Effects from linear mixed models, CBF and volume as dependent variables (stacked), and group (amyloid-β-negative controls versus amyloid-β-positive controls, early and late MCI or Alzheimer's disease with dementia, with amyloid-β standardized uptake value ratio dichotomized by cut-off ⩾1.11) as independent variable, co-varied for age and sex. CBF and volume were residualized by reference CBF (precentral cortex) or intracranial volume, respectively. Tests significant at $P < 0.05$ are printed in bold. Several effects remained significant after correction for multiple comparisons using false discovery rate correction [corrected for 32 tests for volume and 32 for CBF, volume: late MCI entorhinal ($P = 0.01$), hippocampus ($P < 0.001$), Alzheimer's disease entorhinal, hippocampus, and inferior temporal ($P < 0.001$), inferior parietal ($P = 0.006$); CBF: late MCI inferior temporal and inferior parietal ($P = 0.045$), Alzheimer's disease inferior temporal ($P = 0.032$), inferior parietal and precuneus ($P = 0.045$)]. Differences in effects were compared by the interaction between group and imaging modality. No differences were significant when correcting for multiple comparisons using false discovery rate correction (corrected for 32 tests).

the view that in older subjects, the spectrum of cognitive decline can be conceptually dichotomized into those subjects who are amyloid-β-positive and have Alzheimer's disease pathology and those who are not. In regard to this, a previous report showed that ∼30% of subjects with normal cognition, ∼40% of the subjects with early MCI, ∼60% of the subjects with late MCI, and ∼80% of the subjects with Alzheimer's disease were amyloid-β positive in the ADNI cohort, and increased amyloid-β load was related to cognitive dysfunction in early and late MCI (the same subjects as in the present study) (Landau *et al*., 2012).

The third major finding of this study is that amyloid-β pathology has different associations with CBF and structural measurements. In the control population, the amyloid-β load was related to reduced CBF in entorhinal, inferior temporal and inferior parietal regions, whereas effects on grey matter volume were small or positive. But when comparing amyloid-β negative controls with amyloid-β-positive late MCI or Alzheimer's disease, effects of amyloid-β on structure dominated, with greater reductions in volume than in CBF in the advanced disease stages. Although the differences in early stages were mild, and did not reach statistical significance ($P < 0.05$) for most regions, the result is consistent with the long-held view that one of the earliest changes in Alzheimer's disease is synaptic loss (Terry *et al*., 1991) leading to deafferentation and reduction in brain activity, which is reflected in reduced CBF. A previous study found greater reduction of CBF than grey matter volume in inferior temporal areas in Alzheimer's disease (Alsop *et al*., 2008), and one fluorodeoxyglucose PET study showed that hypometabolism was greater than volume loss in MCI and Alzheimer's disease (De Santi *et al*., 2001). Some studies have found higher diagnostic accuracy for

Alzheimer's disease using ASL CBF compared with structural MRI (Raji *et al*., 2010; Dashjamts *et al*., 2011). It should be emphasized that the majority of fluorodeoxyglucose PET and ASL studies have reported data without correcting for the effects of partial volume. In these cases, the results showed the effects of reduced perfusion or metabolism together with the effects of grey matter loss. In contrast, the present study reports all ASL CBF data corrected for both the effects of atrophy and grey matter/white matter. This adds emphasis to the view that the earliest changes of Alzheimer's disease (seen in cognitively healthy controls) may be manifested by reduced CBF, before development of grey matter atrophy. However, this was a cross-sectional study, and longitudinal studies are needed to fully determine if regional changes in CBF appear ahead of changes in volume. This is especially true as the conclusions may be influenced by the technical aspects of the measurement, including differences in precision between the different imaging modalities.

Some limitations of this study ought to be considered: we used pulsed ASL, which often yields lower sensitivity than continuous ASL methods and is also potentially more confounded by variations in arterial transient time, although an ASL study, using more elaborate measurements, found reduced CBF in patients with Alzheimer's disease without reductions in arterial transit times (Yoshiura *et al*., 2009). Nonetheless, it is possible that ASL studies using continuous labelling may lead to different results. Also, our use of distortion correction does not resolve potential signal aliasing, although one would expect that any error in ASL as a result of signal aliasing affects all groups equally and hence would mainly reduce sensitivity of ASL but not mimic a group effect. To reduce the number of statistical tests, we merged data from right and left hemispheres, thereby ignoring potential laterality in alterations that might have biased our results (Alexopoulos *et al*., 2012). A complication that potentially limited sensitivity is that we used anatomically defined regions of interest for both CBF and structural changes whereas functionally defined regions of interest (i.e. Brodmann areas) might have been more effective for capturing regional variations in CBF. However, one strength of our approach is that we considered partial volume effects and effects of grey/white matter on the ASL signal. Tissue partial volume correction of CBF used information from segmented structural MRI data and was based on various assumptions, including linear relationships between CBF and tissue variations and a pre-determined global CBF ratio of white matter/grey matter. To the extent that the segmentation has errors and the assumptions are too restrictive, changes in CBF may be overestimated. Another limitation of this study is that we used a global measurement of amyloid-β pathology, which does not allow direct assessment of local effects of amyloid-β. It should also be stressed that this was a cross-sectional study, where we considered amyloid-β-positive controls, and patients with early and late MCI as likely to represent preclinical and early clinical stages of Alzheimer's disease. However, it is possible that these groups contained a proportion of individuals who will not develop dementia as a result of Alzheimer's disease, and it is also possible that some of the amyloid-β-negative controls, individuals with early or late MCI may go on to develop dementia because of Alzheimer's disease, which may skew the results of any biomarker test intended to measure incipient Alzheimer's disease pathology (including volume and CBF measurements). Finally, some of the tests were done on small groups with measurements with large variances, which may result in low power to detect significant effects. This should be taken into account when interpreting some of the tests with *P*-values slightly above 0.05.

Our study does not explain the mechanisms that lead to CBF alterations in the presence of brain amyloid. Longitudinal studies on subjects with no or minimal cognitive impairment are needed to resolve if loss of CBF is a cause or a consequence of other pathological events in Alzheimer's disease, including amyloid-β accumulation (Austin *et al*., 2011). It is worth mentioning in this context that one recent ASL study found that donepezil treatment increased CBF in middle and posterior cingulate cortex in Alzheimer's disease, suggesting that the detected reductions are at least partially reversible (Li *et al*., 2012).

To conclude, we found that brain amyloid-β load has significant associations with the regional CBF pattern. These associations are detectable at an early stage of amyloid-β pathology in the absence of clinical dementia. Furthermore, the finding that amyloid-β has different associations with CBF and volume, with more pronounced reductions in CBF in cognitively healthy control subjects, is consistent with the view that functional and synaptic loss is an early event in Alzheimer's disease pathology, leading to reduced CBF before grey matter loss. Therefore, measurements of CBF with ASL as part of a MRI protocol may be a sensitive method to detect early Alzheimer's disease pathology and to measure effects of early treatment.

Funding

Data collection and sharing for this project was funded by the Alzheimer's Disease Neuroimaging Initiative (National Institutes of Health Grant U01 AG024904). ADNI is funded by the National Institute on Ageing, the National Institute of Biomedical Imaging and Bioengineering, and through generous contributions from the following: Abbott; Alzheimers Association; Alzheimers Drug Discovery Foundation; Amorfix Life Sciences Ltd.; AstraZeneca; Bayer HealthCare; BioClinica, Inc.; Biogen Idec Inc.; Bristol-Myers Squibb Company; Eisai Inc.; Elan Pharmaceuticals Inc.; Eli Lilly and Company; F. Hoffmann-La Roche Ltd and its affiliated company Genentech, Inc.; GE Healthcare; Innogenetics, N.V.; IXICO Ltd.; Janssen Alzheimer Immunotherapy Research and Development, LLC.; Johnson and Johnson Pharmaceutical Research and Development LLC.; Medpace, Inc.; Merck and Co., Inc.; Meso Scale Diagnostics, LLC.; Novartis Pharmaceuticals Corporation; Pfizer Inc.; Servier; Synarc Inc.; and Takeda Pharmaceutical Company. The Canadian Institutes of Health Research is providing funds to support ADNI clinical sites in Canada. Private sector contributions are facilitated by the Foundation for the National Institutes of Health (www.fnih.org). The grantee organization is the Northern California Institute for Research and Education. ADNI data are disseminated by the Laboratory for Neuro Imaging at the University of California, Los Angeles. This research was also supported by NIH grants P30 AG010129 and K01 AG030514.This research was also supported

by the Swedish Research Council, Goteborgs Lakaresallskap, Svenska Lakaresallskapet, Sahlgrenska Universitetssjukhuset, Carl-Bertil Laurells fond, and Klinisk Biokemi i Norden.

Conflicts of interest

N.M., P.I., D.T., A.S., M.D., W.J. and N.S. report no conflicts of interest. C.R.J. provides consulting services for Siemens Healthcare and Janssen Research and Development L.L.C. He receives research funding from the National Institutes of Health (R01-AG011378, RO1-AG041851, RO1-AG037551, U01-HL096917, U01-AG032438, U01-AG024904), and the Alexander Family Alzheimer's Disease Research Professorship of the Mayo Foundation. L.A.B. has been a consultant for F. Hoffmann-LaRoche Ltd. M.W. has been on scientific advisory boards for Pfizer and BOLT Inter-national; has been a consultant for Pfizer Inc., Janssen, KLJ Associates, Easton Associates, Harvard University, inThought, INC Research, Inc., University of California, Los Angeles, Alzheimer's Drug Discovery Foundation and Sanofi-Aventis Groupe; has received funding for travel from Pfizer, AD PD meeting, Paul Sabatier University, Novartis, Tohoku University, MCI Group, France, Travel eDreams, Inc., Neuroscience School of Advanced Studies (NSAS), Danone Trading, BV, CTAD ANT Congres; serves as an associate editor of Alzheimer's & Dementia; has received honoraria from Pfizer, Tohoku University, and Danone Trading, BV; has research support from Merck, Avid, DOD and VA; and has stock options in Synarc and Elan.

Supplementary material

Supplementary material is available at *Brain* online.

Appendix 1

Data used in preparation of this article were obtained from the Alzheimer's Disease Neuroimaging Initiative (ADNI) database (adni.loni.usc.edu). As such, the investigators within the ADNI contributed to the design and implementation of ADNI and/or provided data but did not participate in analysis or writing of this report. A complete listing of ADNI investigators can be found at: http://adni.loni.usc.edu/wp-content/uploads/how_to_apply/ADNI_Acknowledgement_List.pdf.

References

Alexopoulos P, Sorg C, Förschler A, Grimmer T, Skokou M, Wohlschläger A, et al. Perfusion abnormalities in mild cognitive impairment and mild dementia in Alzheimer's disease measured by pulsed arterial spin labeling MRI. Eur Arch Psychiatry Clin Neurosci 2012; 262: 69–77.

Alsop DC, Detre JA, Grossman M. Assessment of cerebral blood flow in Alzheimer's disease by spin-labeled magnetic resonance imaging. Ann Neurol 2000; 47: 93–100.

Alsop DC, Casement M, de Bazelaire C, Fong T, Press DZ. Hippocampal hyperperfusion in Alzheimer's disease. Neuroimage 2008; 42: 1267–74.

Alsop DC, Dai W, Grossman M, Detre JA. Arterial spin labeling blood flow MRI: its role in the early characterization of Alzheimer's disease. J Alzheimers Dis 2010; 20: 871–80.

Archer HA, Edison P, Brooks DJ, Barnes J, Frost C, Yeatman T, et al. Amyloid load and cerebral atrophy in Alzheimer's disease: an 11C-PIB positron emission tomography study. Ann Neurol 2006; 60: 145–7.

Austin BP, Nair VA, Meier TB, Xu G, Rowley HA, Carlsson CM, et al. Effects of hypoperfusion in Alzheimer's disease. J Alzheimers Dis 2011; 26 (Suppl 3): 123–33.

Bangen KJ, Restom K, Liu TT, Wierenga CE, Jak AJ, Salmon DP, et al. Assessment of Alzheimer's disease risk with functional magnetic resonance imaging: an arterial spin labeling study. J Alzheimers Dis 2012; 31 (Suppl 3): S59–74.

Bateman RJ, Xiong C, Benzinger TL, Fagan AM, Goate A, Fox NC, et al. Clinical and biomarker changes in dominantly inherited Alzheimer's disease. N Engl J Med 2012; 367: 795–804.

Binnewijzend MAA, Kuijer JPA, Benedictus MR, van der Flier WM, Wink AM, Wattjes MP, et al. Cerebral blood flow measured with 3D pseudocontinuous arterial spin-labeling MR imaging in Alzheimer disease and mild cognitive impairment: a marker for disease severity. Radiology 2013; 267: 221–30.

Blennow K, de Leon MJ, Zetterberg H. Alzheimer's disease. Lancet 2006; 368: 387–403.

Chao LL, Pa J, Duarte A, Schuff N, Weiner MW, Kramer JH, et al. Patterns of cerebral hypoperfusion in amnestic and dysexecutive MCI. Alzheimer Dis Assoc Disord 2009; 23: 245–52.

Chao LL, Buckley ST, Kornak J, Schuff N, Madison C, Yaffe K, et al. ASL perfusion MRI predicts cognitive decline and conversion from MCI to dementia. Alzheimer Dis Assoc Disord 2010; 24: 19–27.

Chételat G, Desgranges B, de la Sayette V, Viader F, Eustache F, Baron J-C. Mild cognitive impairment: Can FDG-PET predict who is to rapidly convert to Alzheimer's disease? Neurology 2003; 60: 1374–7.

Chételat G, Villemagne VL, Bourgeat P, Pike KE, Jones G, Ames D, et al. Relationship between atrophy and β-amyloid deposition in Alzheimer disease. Ann Neurol 2010; 67: 317–24.

Cohen AD, Price JC, Weissfeld LA, James J, Rosario BL, Bi W, et al. Basal cerebral metabolism may modulate the cognitive effects of Abeta in mild cognitive impairment: an example of brain reserve. J Neurosci 2009; 29: 14770–8.

Dai W, Lopez OL, Carmichael OT, Becker JT, Kuller LH, Gach HM. Mild cognitive impairment and alzheimer disease: patterns of altered cerebral blood flow at MR imaging. Radiology 2009; 250: 856–66.

Dashjamts T, Yoshiura T, Hiwatashi A, Yamashita K, Monji A, Ohyagi Y, et al. Simultaneous arterial spin labeling cerebral blood flow and morphological assessments for detection of Alzheimer's disease. Acad Radiol 2011; 18: 1492–9.

Detre JA, Leigh JS, Williams DS, Koretsky AP. Perfusion imaging. Magn Reson Med 1992; 23: 37–45.

Dougall NJ, Bruggink S, Ebmeier KP. Systematic review of the diagnostic accuracy of 99mTc-HMPAO-SPECT in dementia. Am J Geriatr Psychiatry 2004; 12: 554–70.

Fink GR, Pawlik G, Stefan H, Pietrzyk U, Wienhard K, Heiss WD. Temporal lobe epilepsy: evidence for interictal uncoupling of blood flow and glucose metabolism in temporomesial structures. J Neurol Sci 1996; 137: 28–34.

Fleisher AS, Podraza KM, Bangen KJ, Taylor C, Sherzai A, Sidhar K, et al. Cerebral perfusion and oxygenation differences in Alzheimer's disease risk. Neurobiol Aging 2009; 30: 1737–48.

Friedland RP, Budinger TF, Ganz E, Yano Y, Mathis CA, Koss B, et al. Regional cerebral metabolic alterations in dementia of the Alzheimer type: positron emission tomography with [18F]fluorodeoxyglucose. J Comput Assist Tomogr 1983; 7: 590–8.

Friedland RP, Jagust WJ, Huesman RH, Koss E, Knittel B, Mathis CA, et al. Regional cerebral glucose transport and utilization in Alzheimer's disease. Neurology 1989; 39: 1427–34.

Hardy J, Selkoe DJ. The amyloid hypothesis of Alzheimer's disease: progress and problems on the road to therapeutics. Science 2002; 297: 353–6.

Ishii K, Sasaki M, Yamaji S, Sakamoto S, Kitagaki H, Mori E. Demonstration of decreased posterior cingulate perfusion in mild Alzheimer's disease by means of H215O positron emission tomography. Eur J Nucleic Med 1997; 24: 670–3.

Jack CR Jr, Knopman DS, Jagust WJ, Petersen RC, Weiner MW, Aisen PS, et al. Tracking pathophysiological processes in Alzheimer's disease: an updated hypothetical model of dynamic biomarkers. Lancet Neurol 2013; 12: 207–16.

Jack CR Jr, Vemuri P, Wiste HJ, Weigand SD, Aisen PS, Trojanowski JQ, et al. Evidence for ordering of Alzheimer disease biomarkers. Arch Neurol 2011; 68: 1526–35.

Jagust WJ, Mormino EC. Lifespan brain activity, β-amyloid, and Alzheimer's disease. Trends Cogn Sci 2011; 15: 520–6.

Johnson KA, Mueller ST, Walshe TM, English RJ, Holman BL. Cerebral perfusion imaging in Alzheimer's disease. Use of single photon emission computed tomography and iofetamine hydrochloride I 123. Arch Neurol 1987; 44: 165–8.

Johnson NA, Jahng G-H, Weiner MW, Miller BL, Chui HC, Jagust WJ, et al. Pattern of cerebral hypoperfusion in Alzheimer disease and mild cognitive impairment measured with arterial spin-labeling MR imaging: initial experience. Radiology 2005; 234: 851–9.

Kim SM, Kim MJ, Rhee HY, Ryu C-W, Kim EJ, Petersen ET, et al. Regional cerebral perfusion in patients with Alzheimer's disease and mild cognitive impairment: effect of APOE epsilon4 allele. Neuroradiology 2013; 55: 25–34.

Landau SM, Mintun MA, Joshi AD, Koeppe RA, Petersen RC, Aisen PS, et al. Amyloid deposition, hypometabolism, and longitudinal cognitive decline. Ann Neurol 2012; 72: 578–86.

Li W, Antuono PG, Xie C, Chen G, Jones JL, Ward BD, et al. Changes in regional cerebral blood flow and functional connectivity in the cholinergic pathway associated with cognitive performance in subjects with mild Alzheimer's disease after 12-week donepezil treatment. Neuroimage 2012; 60: 1083–91.

Luh WM, Wong EC, Bandettini PA, Hyde JS. QUIPSS II with thin-slice TI1 periodic saturation: a method for improving accuracy of quantitative perfusion imaging using pulsed arterial spin labeling. Magn Reson Med 1999; 41: 1246–54.

Matsuda H. Role of Neuroimaging in Alzheimer's Disease, with Emphasis on Brain Perfusion SPECT. J Nucleic Med 2007; 48: 1289–300.

Mosconi L, Tsui W-H, De Santi S, Li J, Rusinek H, Convit A, et al. Reduced hippocampal metabolism in MCI and AD: automated FDG-PET image analysis. Neurology 2005; 64: 1860–7.

Mosconi L, Tsui WH, Herholz K, Pupi A, Drzezga A, Lucignani G, et al. Multicenter standardized 18F-FDG PET diagnosis of mild cognitive impairment, Alzheimer's disease, and other dementias. J Nucleic Med 2008; 49: 390–8.

Oh H, Habeck C, Madison C, Jagust W. Covarying alterations in Aβ deposition, glucose metabolism, and gray matter volume in cognitively normal elderly. Hum Brain Mapp 2014; 35: 297–308.

Ossenkoppele R, Madison C, Oh H, Wirth M, van Berckel BNM, Jagust WJ. Is verbal episodic memory in elderly with amyloid deposits preserved through altered neuronal function? Cereb Cortex 2013.

Ossenkoopele et al. Cereb Cortex 2013, [Epub ahead of print], doi: 10.1093/cercor/bht076, First published online: March 28, 2013.

Raji CA, Lee C, Lopez OL, Tsay J, Boardman JF, Schwartz ED, et al. Initial experience in using continuous arterial spin-labeled MR imaging for early detection of Alzheimer disease. AJNR Am J Neuroradiol 2010; 31: 847–55.

Reiman EM, Caselli RJ, Yun LS, Chen K, Bandy D, Minoshima S, et al. Preclinical evidence of Alzheimer's disease in persons homozygous for the epsilon 4 allele for apolipoprotein E. N Engl J Med 1996; 334: 752–8.

Roberts DA, Detre JA, Bolinger L, Insko EK, Leigh JS Jr. Quantitative magnetic resonance imaging of human brain perfusion at 1.5 T using steady-state inversion of arterial water. Proc Natl Acad Sci USA 1994; 91: 33–7.

De Santi S, de Leon MJ, Rusinek H, Convit A, Tarshish CY, Roche A, et al. Hippocampal formation glucose metabolism and volume losses in MCI and AD. Neurobiol Aging 2001; 22: 529–39.

Schuff N, Matsumoto S, Kmiecik J, Studholme C, Du A, Ezekiel F, et al. Cerebral blood flow in ischemic vascular dementia and Alzheimer's disease, measured by arterial spin-labeling magnetic resonance imaging. Alzheimers Dement 2009; 5: 454–62.

Silverman DH, Small GW, Chang CY, Lu CS, Kung De Aburto MA, Chen W, et al. Positron emission tomography in evaluation of dementia: regional brain metabolism and long-term outcome. JAMA 2001; 286: 2120–7.

Sojkova J, Beason-Held L, Zhou Y, An Y, Kraut MA, Ye W, et al. Longitudinal cerebral blood flow and amyloid deposition: an emerging pattern? J Nucleic Med 2008; 49: 1465–71.

Tao R, Fletcher PT, Gerber S, Whitaker RT. A variational image-based approach to the correction of susceptibility artifacts in the alignment of diffusion weighted and structural MRI. Inf Process Med Imaging 2009; 21: 664–75.

Terry RD, Masliah E, Salmon DP, Butters N, DeTeresa R, Hill R, et al. Physical basis of cognitive alterations in Alzheimer's disease: synapse loss is the major correlate of cognitive impairment. Ann Neurol 1991; 30: 572–80.

Wolk DA, Detre JA. Arterial spin labeling MRI: an emerging biomarker for Alzheimer's disease and other neurodegenerative conditions. Curr Opin Neurol 2012; 25: 421–8.

Xu G, Antuono PG, Jones J, Xu Y, Wu G, Ward D, et al. Perfusion fMRI detects deficits in regional CBF during memory-encoding tasks in MCI subjects. Neurology 2007; 69: 1650–56.

Yoshiura T, Hiwatashi A, Yamashita K, Ohyagi Y, Monji A, Takayama Y, et al. Simultaneous measurement of arterial transit time, arterial blood volume, and cerebral blood flow using arterial spin-labeling in patients with Alzheimer disease. AJNR Am J Neuroradiol 2009; 30: 1388–93.